Natural Hazards (2025) 121:11051–11078
https://doi.org/10.1007/s11069-025-07234-y

ORIGINAL PAPER

Drought analysis based on nonparametric multivariate standardized drought index in the Seyhan River Basin

Tolga Barış Terzi[1] · **Bihrat Önöz**[2]

Received: 6 July 2024 / Accepted: 8 March 2025 / Published online: 3 April 2025

Abstract

Drought is a detrimental natural hazard that is a threat to the social and ecological aspects of life. Unlike other natural hazards, drought occurs slowly and gradually, making it difficult to detect its formation, leading to severe consequences in the affected area. Therefore, precise and reliable monitoring of drought is crucial to implement effective drought mitigation strategies. Drought indices are significant tools for drought monitoring; single variable indices are quite frequently used in the literature to assess drought conditions. Although these indices are generally accurate at characterizing the specific type of drought they were developed for, they fail to provide a comprehensive representation of drought conditions. Hence, this study applies a nonparametric multivariate standardized drought index (MSDI) that integrates meteorological and hydrological drought to investigate the dynamics of drought events within the Seyhan River Basin (SRB). Trend analyses were conducted to detect any directional changes in the drought patterns within the SRB. Additionally, this study examined the potential effects of El Nino-Southern Oscillation events on the MSDI series to determine their impact on drought conditions in the SRB. The results indicate that the MSDI outperforms the single variable indices in characterizing drought conditions within the basin. The calculations conducted for 5 different time scales 1, 3, 6, 9 and 12-months showed satisfactory results in multivariate analysis of drought. Upon examining the trend analyses, MSDI series showed an insignificant negative trend in all stations within the SRB. The MSDI series was strongly influenced by Nino 3.4 and Arctic Oscillation (AO) indices while sunspot activities had a relatively weak impact on the MSDI series.

Keywords Drought · Integrated drought index · Multivariate standardized drought index · Standardized precipitation index · Standardized streamflow index

✉ Tolga Barış Terzi
tolgabaristerzi@ktu.edu.tr

Bihrat Önöz
bihrat.onoz@isikun.edu.tr

[1] Department of Civil Engineering, Faculty of Engineering, Karadeniz Technical University, Trabzon, Turkey

[2] Department of Civil Engineering, Faculty of Engineering and Natural Sciences, Işık University, Istanbul, Turkey

1 Introduction

The increasing impacts of natural hazards such as drought are significantly affected by the intensifying effects of climate change (IPCC 2012). Climate models consistently predict a further intensification of these impacts (Reidmiller et al. 2018). Drought is a natural hazard that occurs slowly and gradually, leading to deficits in water resources (Dracup et al. 1980). Drought events, marked by prolonged periods of precipitation deficits and insufficient water supply, have dire effects on various sectors (Wilhite 2005; Huang et al. 2016; Fang et al. 2018, 2019). With the increasing impacts of climate change and rising water demand across the globe, the effects of droughts become more detrimental, making drought mitigation even more challenging (Pascolini-Campbell et al. 2021; Walker and Van Loon 2023; AghaKouchak et al. 2014). In the twenty-first century droughts have affected nations and regions around the globe to differing extents (Liu et al. 2023; Tripathy and Mishra 2023). Drought events are often complex, characterized by extended durations, and can overlap with multiple types of drought, such as meteorological, agricultural, and hydrological droughts (AghaKouchak et al. 2020). Given its complex nature, drought events depend not only on atmospheric conditions and hydrological processes but also on human and social factors, highlighting the need for a comprehensive understanding and the development of effective mitigation strategies (Mishra and Singh 2010). Since understanding the effects of drought is crucial for risk management, numerous studies have been conducted to develop an effective drought monitoring system (Hao et al. 2017; Ali et al. 2019; Wu et al. 2024; Wang et al. 2023).

Drought indices quantify drought in numerical terms and are essential in analyzing drought situations. These indices provide a more comprehensive representation of drought compared to raw data such as precipitation and streamflow (Wilhite et al. 2000; Keyantash and Dracup 2002). Currently, the literature features a diverse range of drought indices, each representing different types of droughts.

Drought is classified into five different groups: meteorological, hydrological, agricultural, ecological and socioeconomic drought (Wilhite and Glantz 1985; American Meteorological Society 2004). Meteorological drought begins when precipitation falls below normal levels in a region and can lead to hydrological drought that affects environmental functions both ecologically and climatologically (Van Loon and Laaha 2015; Heudorfer and Stahl 2016; Crausbay et al. 2017; Ahmadi et al. 2019). Numerous meteorological drought indices are currently used in the literature, with the Standardized Precipitation Index (SPI; McKee et al. 1993) and the Standardized Precipitation Evapotranspiration Index (SPEI; Vicente-Serrano et al. 2010) being particularly widely used among them. The SPI assesses drought conditions over a period based solely on precipitation deficit whereas SPEI evaluates drought conditions over a period by factoring in both precipitation and potential evapotranspiration, thus accounting for the impact of evapotranspiration on drought (Gumus 2023; Liu et al. 2016a, b). Hydrological drought can be defined as the manifestation of water deficiency in hydrological systems, characterized by low streamflows in rivers, low water levels in lakes, reservoirs, and groundwater sources (Mishra and Singh 2011). Streamflow is commonly employed for developing hydrological drought indices in the literature due to its responsiveness to underlying surface conditions and meteorological variables enabling an accurate portrayal of the hydrological drought status (Wang et al. 2020). Some of the popular indices developed to assess hydrological drought in the literature include the standardized streamflow index (SSFI), the streamflow drought index (SDI), and the surface water supply index (SWSI) (Modarres 2006; Nalbantis and Tsakiris

2008; Shafer and Dezman 1982). Agricultural drought is assessed by examining the relationship between soil moisture levels and plant morphology during growth, reflecting the degree to which soil moisture falls below the minimum requirement for plant sustenance (Liu et al. 2016a, b). In summary, the definition of agricultural drought focuses on the deficit of soil moisture, as well as its consequences on agricultural productivity (Panu and Sharma 2002). Frequently utilized indices for agricultural drought include the normalized vegetation difference index (NDVI), soil moisture deficit index (SMDI), and evapotranspiration deficit index (ETDI) (Carlson et al. 1994; Narasimhan and Srinivasan 2005). However, drought indices based on a single variable can only address a specific aspect of drought, such as meteorological or hydrological (Mishra and Singh 2010). The precipitation deficit is indicative of drought onset and effectively identifies when drought begins. In contrast, the reduction in streamflow, a measure of hydrological drought, is more useful in determining the duration of the drought (Huang et al. 2019). Thus, it is challenging for a single drought index to capture all the different aspects of droughts at once and to represent the drought accurately in an integrated manner (Luo et al. 2023; Hao and AghaKouchak 2013).

Various composite drought indices have been developed to comprehensively investigate drought events (Svoboda et al. 2002; Huang et al. 2014a). The U.S. Drought Monitor (USDM), introduced by Svoboda et al. in 2002, uses data from climate indices, numerical models, and insights provided by experts at both regional and local levels. Keyantash and Dracup (2004) developed the Aggregated Drought Index (ADI) through an analysis of multiple physical variables associated with drought, such as evapotranspiration, precipitation, streamflow, and soil moisture, utilizing principal component analysis (PCA). Nevertheless, these composite indices have their own limitations as the conditions required for PCA may not always be fulfilled in practical scenarios. Most of the composite indices in today's literature have been developed utilizing copulas to measure the combined characteristics of drought events. The joint drought index (JDI) developed by Kao and Govindaraju (2010) has been utilized to quantify drought characteristics using data from precipitation and streamflow. MSDI was also developed by utilizing copulas to determine the drought characteristics based on soil moisture and precipitation data (Hao and AghaKouchak 2013). The characterization of comprehensive drought indices based on copulas maintains the unique features of each drought variable and describes the relationships between them (Luo et al. 2023). Therefore, copula-based comprehensive drought indices have found extensive application in monitoring drought across diverse areas (Varol et al. 2023; Zhang et al. 2017; She and Xia 2017; Suo et al. 2024; Seo et al. 2024).

While the SPI method offers several advantages, including simplicity, standardization, and flexibility (Hao and AghaKouchak 2014; Farahmand and AghaKouchak 2015), it also has notable disadvantages that cannot be overlooked. One significant drawback is the necessity of assuming a PDF when fitting the data time series. Parametric drought indices such as SPI and SSFI operate on the assumption that there is an appropriate probability distribution function (PDF) that accurately represents the data for modeling purposes (Angelidis et al. 2012; Tijdeman et al. 2020). Typically, in the SPI method, hydrometeorological data records are fitted to a PDF—commonly Gamma distribution for precipitation data and Lognormal distribution for streamflow data—though this choice may not always be the most suitable (Guttman 1999; Quiring 2009). Therefore, they are highly influenced by the selected PDF, particularly in the distribution's tail. (Naresh Kumar et al. 2009). In practice, various issues may arise from the assumption that hydrometeorological data should follow a specific distribution function (Zhu et al. 2015).

As a parametric method, copulas also depend on the assumption that datasets conform to certain PDF's (Huang et al. 2014b). However, there isn't a universally agreed-upon parametric distribution for hydrometeorological variables (Smakhtin 2001), and employing such distributions often leads to significant discrepancies in low or high quantiles (Sharma 2000). To overcome these discrepancies, a nonparametric method employing the Gringorten plotting position formula (Gringorten 1963) was introduced for drought monitoring. This method employs a multivariate drought index, which was then evaluated against both the SPI and standardized soil moisture index (SSI) (Hao and AghaKouchak 2014). The findings indicate that this approach surpasses single variable drought indices in detecting drought conditions. Moreover, the Gringorten plotting position formula, reflecting an empirical frequency distribution, can circumvent the need for fitting parametric distributions, thereby mitigating discrepancies in low or high quantiles.

The Seyhan River Basin is highly prone to drought, with its seasonal precipitation and streamflow patterns typical of a Mediterranean climate: wet winters followed by prolonged dry summers. Precipitation and streamflow peak in December and April, respectively, leaving an extended period of low water availability during the summer months (Cavus et al. 2023). Approximately 41% of the basin is actively used for agriculture, with the fertile Çukurova Plain in the south serving as a critical agricultural area for Turkey and one of the most productive regions worldwide (Altın et al. 2019). Droughts in the basin can severely impact agriculture and hydroelectric energy production, both of which rely on consistent water resources, heightening the demand on limited summer water availability (GDWM 2019). A historical drought analysis is essential for this basin, given its substantial role in Turkey's economic and social development (Gumus and Algin 2016).

Past studies on drought in the SRB have provided significant insights into the region's vulnerability to both meteorological and hydrological droughts. Gumus and Algin (2016) used SPI and SDI across 14 meteorological and 12 streamflow stations, revealing a one-year lag between meteorological and hydrological droughts, which can aid in better water resource management. Similarly, Bayer Altın et al. (2019) employed the SDI to examine hydrological droughts over a 43-year period, identifying trends of increasing drought frequency, particularly after 2000, and highlighting the importance of understanding both short-term and long-term drought patterns. Cavus (2019) focused on spatial drought characterization using SPI and precipitation deficit analysis, emphasizing the variability in drought severity across the basin and the importance of spatial analysis for water resource planning. Topçu et al. (2021) applied the ADI to assess meteorological drought in the Eastern Mediterranean, Seyhan, Ceyhan, and Asi Basins, showing that while severe droughts are rare, localized extreme droughts do occur, particularly due to high irrigation demand. Dikici (2022) utilized satellite-based vegetation indices to detect drought trends in the Seyhan Basin, noting a linear increase in drought frequency and a decrease in forestland and agricultural areas, which may exacerbate future drought conditions.

While these studies have advanced our understanding of drought in the SRB, they also underscore some limitations of traditional, single-variable drought indices. Indices like SPI and SDI focus primarily on either meteorological or hydrological conditions, which may provide an incomplete picture when applied individually. For instance, SPI's reliance on precipitation alone may capture drought onset but fail to account for extended impacts on streamflow, whereas SDI, focused on streamflow, may lag in drought detection. These indices often fail to capture the intricate relationship between precipitation and streamflow that defines drought in the SRB, where diverse seasonal patterns and high agricultural demand create complex drought dynamics. Furthermore, because these indices generally rely on

parametric assumptions about data distributions, they may lack flexibility and robustness in regions with variable data, such as the SRB.

Given these limitations, a nonparametric, multivariate approach like the MSDI offers a particularly suitable solution for capturing the SRB's complex drought dynamics. By integrating meteorological and hydrological factors without relying on specific data distributions, the MSDI provides a single, standardized measure that is both adaptable and comprehensive. Unlike other composite indices that depend on parametric methods, MSDI's nonparametric structure circumvents distributional assumptions, making it particularly effective for regions with unique hydrometeorological patterns. This approach not only supports more informed decision-making for drought mitigation but also aligns with the need for a unified index that can enhance water resource management and resilience across key sectors reliant on consistent water availability.

In brief, the present study aims to: (1) Model a nonparametric multivariate standardized drought index (MSDI) based on precipitation and streamflow data, evaluating its reliability and superiority over single variable indices, (2) Analyze the drought characteristics within the SRB, and (3) investigate the relationship between ENSO events and drought characteristics.

2 Study area and data

2.1 Study area

The Seyhan River Basin (SRB) is located in the southern part of Turkey with its upper part located in the Central Anatolia Region, and its middle and lower parts in the Mediterranean Region. It spans between the north latitudes of 36° 30′ and 39° 15′ and the east longitudes of 34° 45′ and 37° 00′. The Seyhan Basin generally has a mountainous terrain. It extends from sea level on the Mediterranean coast in the south to elevations of 3500 m in the Taurus Mountains in the north (Fig. 1). The northern segment of the basin showcases traits akin to the Central Anatolian climate, resulting in comparatively lower temperatures than its southern counterpart. This region experiences the most significant precipitation levels, particularly in its elevated terrains. In the coastal plains of Çukurova and surrounding areas, summers are marked by intense heat and aridity, with rainfall amounts dropping to as low as 10 mm, while winters are mild and receive substantial rainfall, reaching up to 160 mm (SYGM 2019). Between the southern coastal belt and the Tarsus Mountains to the north lies an intermediary zone characterized by a semi-arid Mediterranean climate, marked by dry, sweltering summers and moist, temperate winters (Cavus and Aksoy 2019). The Seyhan River Basin is prone to drought due to its semi-arid climate and human activities.

While the SRB is extensively studied in the literature (Gumus and Algin 2016; Altın et al. 2019; Terzi and Önöz 2024b; Topçu et al. 2021); existing literature lacks comprehensive multivariate analyses of drought in the area. This research gap hinders a deeper understanding of drought dynamics and the development of effective mitigation strategies.

2.2 Data

The monthly precipitation data of 10 meteorological stations in the SRB from 1989 to 2011 were derived from the State Meteorological Service (MGM). The monthly streamflow data

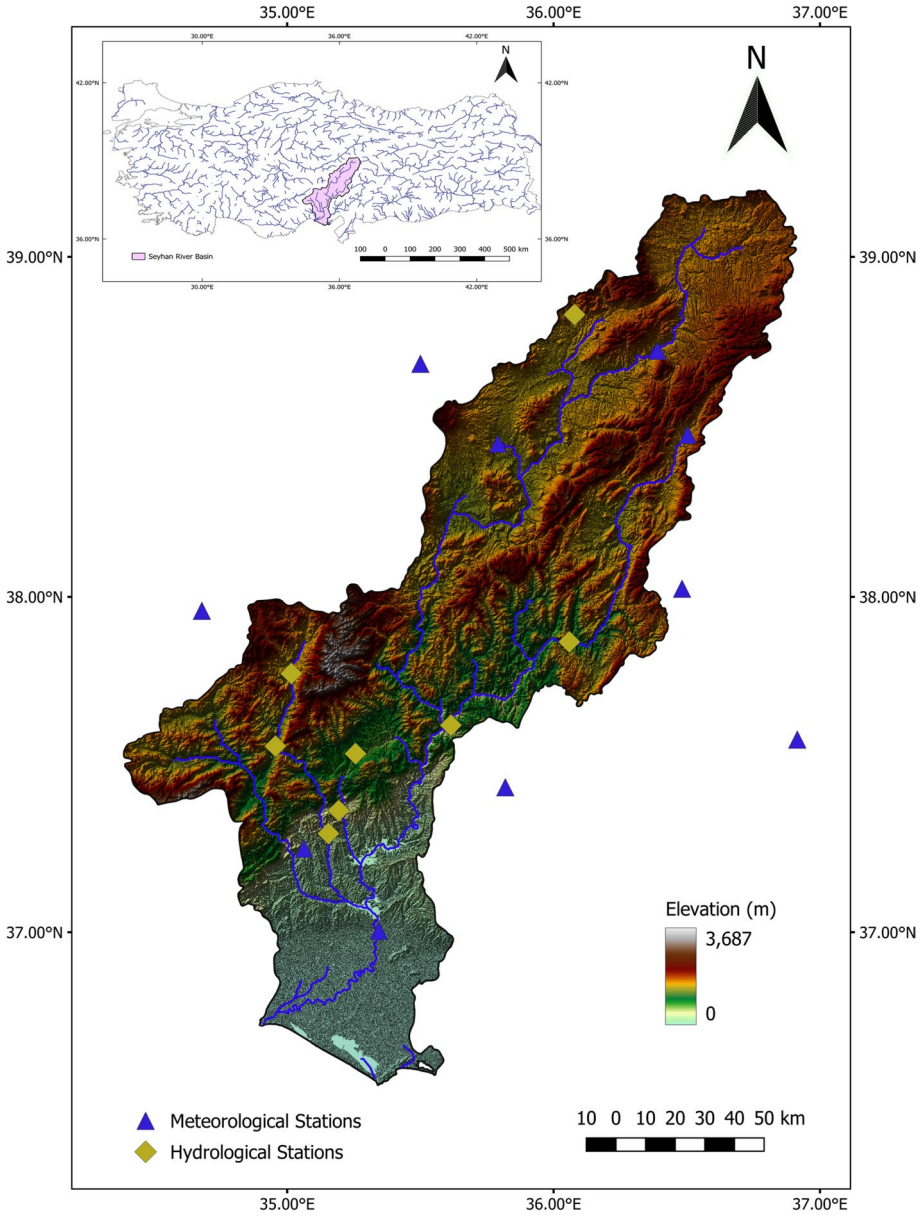

Fig. 1 Topographic map of the SRB

of the hydrological stations in the SRB from 1989 to 2011 were obtained from the General Directorate of State Hydraulic Works (DSI). The details of the hydrological and meteorological stations are shown in Table 1.

The analysis of the precipitation data revealed that it predominantly followed a Gamma distribution, as confirmed by the Kolmogorov–Smirnov (K-S) test, indicating a good fit to the theoretical distribution. In contrast, the streamflow data did not exhibit a significant fit

Table 1 Hydrological and meteorological stations in the SRB

Code	Station name	Latitude	Longtitude	Altitude(m)	Observation period	Selected period
D18A008	Tacin	38.8311	36.0789	1536	1964–2015	1989–2011
D18A012	Kamışlı	37.5500	34.9569	1094	1970–2015	1989–2011
D18A023	Yeniköy	37.5339	35.2567	870	1985–2015	1989–2011
D18A027	Elekgölü	37.7725	35.0155	1550	1986–2015	1989–2011
E1801	Himmetli	37.8664	36.0589	665	1935–2011	1989–2011
E1805	Gökdere	37.6186	35.6144	312	1938–2011	1989–2011
E1820	Hacılı Köprüsü	37.2955	35.1547	167	1968–2011	1989–2011
E1825	Eğribük	37.3639	35.1930	222	1986–2011	1989–2011
17196	Kayseri Bölge	38.6870	35.5000	1093	1960–2016	1989–2011
17250	Niğde	37.9585	34.6795	1211	1960–2012	1989–2011
17255	Kahramanmaraş	37.5760	36.9150	572	1960–2016	1989–2011
17351	Adana Bölge	37.0041	35.3443	23	1960–2016	1989–2011
17802	Pınarbaşı	38.7251	36.3903	1500	1963–2009	1989–2011
17837	Tomarza	38.4522	35.7912	1402	1965–2010	1989–2011
17840	Sarız	38.4781	36.5035	1599	1968–2011	1989–2011
17866	Göksun	38.0240	36.4823	1344	1970–2011	1989–2011
17908	Kozan	37.4337	35.8202	109	1970–2011	1989–2011
17936	Karaisalı	37.2505	35.0628	240	1965–2011	1989–2011

to either the Gamma or Lognormal distributions, with K-S test results showing low p-values, suggesting that neither of these parametric models adequately represented the streamflow characteristics.

The p-values from the K-S test for the streamflow data are presented in Table 2.

Although the rejection of Gamma and Lognormal distributions in the K-S analysis might be due to the dataset's relatively short length, in practice, obtaining long and reliable datasets for hydrological analysis can be challenging, especially when dealing with specific regions or phenomena such as droughts. Many datasets are constrained by the availability of long-term data, making it difficult to apply parametric methods that typically require a larger sample size for robust estimation of distributional parameters. In such cases, nonparametric methods offer significant advantages. They do not rely on assumptions about the underlying distribution of the data, making them more flexible and suitable for shorter datasets. By avoiding the need for fitting specific probability distributions, nonparametric approaches can provide more reliable and robust results in situations where data length is limited.

Consequently, due to the lack of a significant fit, a nonparametric approach was employed in this study to assess drought conditions in the SRB.

Table 2 *p* values of the K-S test for streamflow data

PDF	E1801	E1805	E1820	E1825	D18A008	D18A012	D18A023	D18A027
Gamma	9.40E−10	0.0003	0.0197	3.94E−05	0.8137	0.1979	0.0054	0.0008
Lognormal	0.00025	0.0018	0.4183	0.0011	0.5070	0.6930	0.0014	0.1827

3 Methodology

MSDI is an effective tool for drought monitoring as it integrates both meteorological and hydrological factors, providing a more comprehensive view of the region's water scarcity. In the SRB, our analysis found that streamflow data did not conform to typical parametric distributions, underscoring a limitation of traditional parametric drought indices which assume specific data distributions. The MSDI, however, is nonparametric and thus avoids this limitation, making it a more flexible and robust choice for the SRB's variable hydrometeorological conditions. Its nonparametric nature ensures applicability across all stations in the basin regardless of local data inconsistencies, allowing for straightforward and consistent calculations. By standardizing multiple drought indicators into a single, unified measure, the MSDI provides a clear and accessible overview of drought conditions, facilitating better decision-making in water management and agriculture. This approach mirrors the effectiveness of comprehensive systems like the USDM (Svoboda et al. 2002), where a single index captures overall drought conditions, supporting informed and timely responses. The MSDI's adaptability and simplicity make it an essential tool for cross-regional comparisons and for developing targeted mitigation strategies, addressing the SRB's drought challenges comprehensively and enhancing resilience across sectors reliant on water resources.

The calculation processes for parametric and nonparametric standardized indices, as well as the MSDI, are detailed in the following sections.

3.1 Accumulation of the data

The drought indices in this study are calculated for time scales of 1, 3, 6, 9, and 12 months to facilitate the monitoring of both short-term and long-term drought conditions.

Accumulation of the data over a chosen time scale is performed as follows:

$$X_{acc,ts} = \frac{X_{i-ts+1}+X_{i-ts+2}+\ldots+X_i}{ts} \quad (1)$$

where X is the variable (e.g. precipitation, streamflow) utilized in the calculation of a drought index (e.g. precipitation, streamflow, soil moisture), while ts denotes the chosen time scale (e.g. 1, 3, 6, 9, 12).

3.2 Standardized drought indices

Standardized drought indices, such as the SPI (McKee et al. 1993), SSI (Hao and AghaKouchak 2013), and SSFI (Modarres 2006), are established and well-known indices that have frequently been employed in the literature for drought analysis (Aon and Biswas 2023; Lee et al. 2024; Mukhawana et al. 2024; Terzi and Önöz 2024a; Xu et al. 2018). Most of these indices are developed based on the SPI methodology (McKee et al. 1993) due to its advantages, including its standardization for easy comparison across different locations and time periods, flexibility in calculating various time scales, robust statistical foundation, and widespread acceptance in the scientific community (Hayes et al. 1999). This section provides a comprehensive explanation of the SPI method.

The accumulation of the selected data—precipitation for the SPI, streamflow for the SSFI, and soil moisture for the SSI—is calculated over the chosen time scales as

described in Sect. 3.1. Subsequently, the best-fit probability distribution function is identified for the accumulated data, with the Gamma distribution typically used for the SPI and the Lognormal distribution commonly applied for the SSFI. For the sake of brevity, the remaining processes in the SPI method will be illustrated exclusively for the Gamma distribution.

$$f(x;\alpha,\beta) = \frac{x^{\alpha-1}e^{-\frac{x}{\beta}}}{\beta^{\alpha}\Gamma(\alpha)} \tag{2}$$

Equation (2) presents the probability density function of the Gamma distribution where α denotes the shape parameter, β represents the scale parameter and $\Gamma(\alpha)$ is the Gamma function defined in Eq. (3).

$$\Gamma(\alpha) = \int_0^{\infty} t^{\alpha-1}e^{-t}dt \tag{3}$$

The estimation of parameters for a probability distribution function (PDF) involves the use of the maximum likelihood method (MLE), which maximizes the log-likelihood function of the selected PDF with respect to its parameters. The log-likelihood function for the Gamma distribution is expressed as follows:

$$l(\alpha,\beta) = \sum_{i=1}^{n}\left[(\alpha-1)logx_i - \frac{x_i}{\beta} - \alpha log\beta - log\Gamma(\alpha)\right] \tag{4}$$

The first derivatives of Eq. (4) with respect to parameters α and β are then solved to estimate the parameters.

The dataset is organized then divided into 12 groups, corresponding to individual months or accumulation of months. For each group, the estimated parameters are applied to develop the cumulative probability distribution function. Equation (5) illustrates the cumulative distribution function for the Gamma distribution:

$$F(x;\alpha,\beta) = \frac{\gamma\left(\alpha,\frac{x}{\beta}\right)}{\Gamma(\alpha)} \tag{5}$$

where $\gamma\left(\alpha,\frac{x}{\beta}\right)$ is the lower incomplete Gamma function defined as:

$$\gamma\left(\alpha,\frac{x}{\beta}\right) = \int_0^{\frac{x}{\beta}} t^{\alpha-1}e^{-t}dt \tag{6}$$

When the dataset includes zero values, the cumulative probability distribution outlined in Eq. (5) is not applicable. To resolve this, an adjustment to the cumulative probabilities is needed. The formula for the adjusted cumulative probability is as follows:

$$H(x) = q + (1-q)F(x) \tag{7}$$

In Eq. (7), $F(x)$ represents the cumulative probability, and q denotes the probability of zero precipitation. This adjustment ensures that the cumulative probability distribution reflects the presence of zero values in the dataset, resulting in a more accurate representation of the distribution.

The cumulative probabilities are subsequently standardized using the inverse of the standard normal distribution function, which has a mean of zero and a standard deviation of one. The standardization formula is as follows:

$$SPI = \phi^{-1}(H(x)) \tag{8}$$

3.3 Nonparametric standardized drought indices

Given the limitations of parametric methods discussed in Sect. 1, this study opts for empirical probabilities to establish a nonparametric standardized index (Farahmand and AghaKouchak 2015). This approach entails establishing the marginal probabilities of precipitation and streamflow using the Gringorten plotting position formula as shown in Eq. (9) (Gringorten 1963):

$$p\left(x_i\right) = \frac{i-0.44}{n+0.12} \tag{9}$$

In Eq. (9) n denotes the number of observed data while i represents the rank of precipitation data from the smallest.

Following a similar methodology as the SPI method, the nonparametric method for calculating the standardized drought indices derives probabilities from Eq. (9). The output of Eq. (9) is then used as an input in Eq. (10) to compute the nonparametric Standardized Index (SI):

$$SI = \phi^{-1}(p) \tag{10}$$

The symbol ϕ denotes the standard normal distribution function, while p represents the calculated joint probability.

Single variable indices were computed for 1, 3, 6, 9, and 12-month periods using both parametric and empirical methods in this study. To further investigate drought characteristics comprehensively, MSDI was computed for the aforementioned periods.

3.4 Multivariate standardized drought index (MSDI)

The joint probability of selected precipitation and streamflow data is described in the Eq. (11), where accumulated precipitation and streamflow data for the time chosen time scale are denoted by X and Y, respectively.

$$P(X \leq x, Y \leq y) = p \tag{11}$$

In the Eq. (11) p denotes the joint probability of the selected data. MSDI then can be defined on joint probability of selected hydrometeorological variables (precipitation and streamflow) by utilizing the inverse of a standard normal distribution as shown in the Eq. (12) (Hao and AghaKouchak 2013):

$$MSDI = \phi^{-1}(p) \tag{12}$$

MSDI, calculated based on the joint probability of the X (precipitation) and Y (streamflow) using the standard normal distribution function (ϕ), provides insights into drought conditions across time spans of 1, 3, 6, and 12 months (Hao and AghaKouchak 2014).

Hao and AghaKouchak (2013), described the joint probability distribution in Eq. (11) by utilizing parametric copula functions as per Nelsen (2006). Although copula functions are frequently used in drought studies to describe the inter-correlation between hydrometeorological variables, they also exhibit several disadvantages. As parametric

approaches, copulas rely on the premise that the selected data fit a specific PDF, which requires accurate parameter estimations (Huang et al. 2016). To avoid discrepancies and the complexities associated with parameter estimations, this study utilizes a nonparametric approach based on empirical joint probability (Hao and AghaKouchak 2014).

In the case of bivariate analysis, the empirical joint probability can be estimated using a modified version of the Gringorten plotting position formula, as proposed by Gringorten in 1963:

$$P\left(x_k, y_k\right) = \frac{(m_k - 0.44)}{(n + 0.12)} \tag{13}$$

In Eq. (13), n denotes the number of observed precipitation and streamflow data while m_k represents the number of occurrences of the (x_i, y_i) pair such that both x_i is less than or equal to x_k and y_i is less than or equal to y_k. The output of the Eq. (13) will then be used as an input for Eq. (12) to calculate the MSDI series.

The primary distinction between Eq. (9) and Eq. (13) is that Eq. (13) extends the concept of the Gringorten plotting position (Gringorten 1963) to the realm of bivariate frequency analysis, wherein two variables are considered concurrently. Specifically, Eq. (13) focuses on assigning joint probabilities to each pair of observations, thereby capturing the dependence structure that exists between the two variables. This extension is crucial for understanding the interactions between the variables, allowing for a more comprehensive analysis of their joint behavior in scenarios where both variables are relevant.

3.5 The modified Mann–Kendall (MMK) trend test

Various statistical tests exist for analyzing trends, with the nonparametric and distribution-free Mann–Kendall (Mann 1945; Kendall 1955) test being recommended by the World Meteorological Organization. The Mann–Kendall test remains effective even in the presence of outliers and non-linear trends within the time series (Önöz and Bayazit 2003). Hamed and Rao (1998) adjusted the Mann–Kendall test to account for the potential influence of positive or negative autocorrelation in the observed data, thereby reducing the likelihood of erroneously identifying a trend as statistically significant at the predetermined level. The correlation analysis reveals notable autocorrelation within the MSDI series at the relevant time scale in the study region. Therefore, this study utilizes the MMK test to ascertain trends within the MSDI series.

For a sequence of n observations over time, the trend statistic S is calculated in the following manner:

$$S = \sum_{i<j} sgn\left(x_j - x_i\right) \tag{14}$$

where

$$sgn\left(x_j - x_i\right) = \begin{cases} 1 & x_j > x_i \\ 0 & x_j = x_i \\ -1 & x_j < x_i \end{cases} \tag{15}$$

Kendall (1955) proposed the variance of trend statistic S as shown in Eq. (16).

$$Var(S) = \frac{n(n-1)(2n-5)}{18} \tag{16}$$

The standardized test statistic Z, derived from the standard normal distribution at the specified significance level α, is computed to assess the significance of the trend in the time series as shown in Eq. (17).

$$Z = \frac{S}{Var(S)^{\alpha}} \tag{17}$$

Significant autocorrelations within a time series can disturb the accurate assessment of the variance of S represented by $Var(S)$ in Eq. (17). To mitigate the impact of this persistence, a nonparametric trend estimator could directly be derived from the original time series (Hamed and Rao 1998). This estimator assists in calculating the autocorrelation coefficients of the new time series, which are then ranked according to their magnitude.

$$V^{*}(S) = Var(S)Cor \tag{18}$$

In Eq. (18), Cor is the correction factor accounting for the autocorrelation in the time series, and is computed in the following manner:

$$Cor = 1 + \frac{2}{n(n-1)(n-2)} \sum_{i=1}^{n-1} (n-1)(n-i-1)(n-i-2)\rho_s(i) \tag{19}$$

3.6 Cross-wavelet analysis

Cross-wavelet analysis is a powerful tool used to examine the relationship between two time series in both time and frequency domains. It allows for the identification of common power and phase relationships at different frequencies, which can reveal underlying interactions. This method is particularly useful in studying complex environmental processes, such as drought patterns, where multiple variables interact over time (Aon and Biswas 2023). The cross-wavelet transformation of two time series x_n and y_n is denoted as $W^{XY} = W^X W^{Y*}$, where W^X and W^Y are the wavelet transforms of each series and the symbol * represents the complex conjugation operation applied to one of the wavelet transforms.

The cross-wavelet power, represented as $|W^{XY}|$, highlights areas in time–frequency field where two series exhibit significant common power. In addition to power, the phase relationship between the two series is crucial for understanding how they interact. The phase, represented by the complex argument of W^{xy}, provides insight into whether the series are in phase, out of phase, or if one series leads or lags the other at specific frequencies (Aon et al. 2024; Huang et al. 2015).

Since the time series are finite in length and wavelets are not fully localized in time, boundary effects at the beginning and end of the series can cause inaccuracies in the cross-wavelet transform. To account for these issues, the cone of influence (COI) is introduced. The COI identifies regions in the time–frequency domain where edge effects are significant, providing guidance on which areas of the results can be considered reliable (Aon and Biswas 2024). By incorporating the COI, the analysis ensures more accurate interpretation of the phase and power relationships, particularly at the boundaries of the data.

In cross-wavelet analysis, the term significant frequency refers to frequency bands where the cross-wavelet power is statistically significant. These significant frequencies indicate

the predominant periods at which the two series are highly correlated over time. Statistical significance is assessed by comparing the observed cross-wavelet power against a background noise model, such as red noise, to identify frequencies that stand out as being genuinely related rather than due to random variability. Identifying these significant frequencies is crucial for understanding the temporal dynamics and commonalities between the series.

Further details of the cross-wavelet analysis and the relevant Matlab code can be found in the following website: http://noc.ac.uk/using-science/crosswavelet-wavelet-coherence (Grinsted et al. 2004).

4 Results

One of the purposes of the present study is to assess the accuracy of the developed MSDI in the SRB by comparing it with traditional single variable drought indices, given that these single variable indices are widely employed in literature, with some being recommended by the World Meteorological Organization (WMO) due to their proven reliability in drought monitoring, as evidenced by previous studies.

The findings are presented in the following sections.

4.1 Performance of the constructed MSDI

The MSDI, SPI, and SSFI datasets for 1-, 3-, 6-, 9- and 12-month time scales spanning from 1989 to 2011 for station D18A027 were graphed and illustrated in Fig. 2. The figure demonstrates that the fluctuation trend observed in MSDI aligns closely with those of SPI and SSFI, suggesting that the synthesized MSDI effectively encapsulates the variations in SPI and SSFI, thus representing the combined characteristics of both meteorological and hydrological droughts. Notably, the values of MSDI are generally lower than those of the single variable indices, indicating that the drought conditions represented by the MSDI are typically more severe than those represented by single variable indices.

It is evident from Fig. 2. that the MSDI effectively integrates the strengths of both SPI and SSFI, precisely delineating the onset and end of each drought event. It is noteworthy that parametric and empirical indices often exhibit disparities, particularly at the extreme ends of data distributions. Parametric indices, which aim to model data by assuming specific probability distributions, may display significant differences, especially in the tail ends (Quiring 2009). These discrepancies tend to become more pronounced as the mismatch between data distribution and assumed distribution increases. In contrast, empirical indices are not reliant on specific distribution assumptions and therefore are less susceptible to such discrepancies.

In general, these indices exhibit similar temporal trends. Table 3 displays the Pearson correlation coefficients between SPI, SSFI, and MSDI at 12-month time scale. The data suggests that using MSDI for drought characterization and monitoring can be considered reliable. Table 3 reveals that all correlation coefficients were greater than 0.70, with the majority exceeding 0.75. This suggests that the developed MSDI exhibits reliability when compared with other drought indices.

By integrating data on both precipitation and streamflow, MSDI proves to be more adept at characterizing genuine drought conditions within a watershed compared to single variable indices.

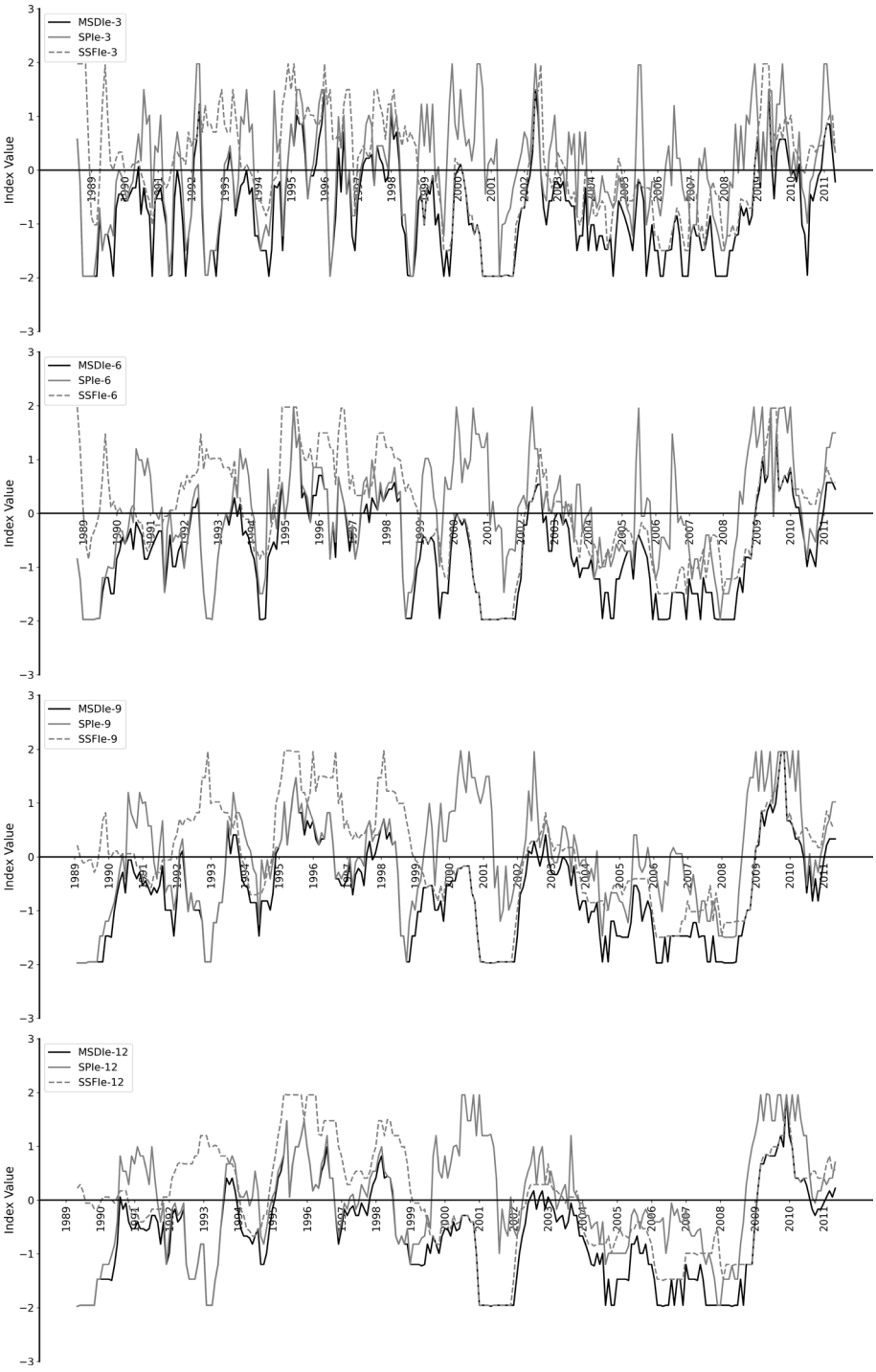

Fig. 2 Comparison of single variable indices and MSDI for station D18A027 from 1989 to 2011

Table 3 Correlation coefficients between the MSDI and single variable indices in the SRB

Index	D18A008	D18A012	D18A023	D18A027	E1801	E1805	E1820	E1825
SPIp	0.80	0.73	0.77	0.73	0.80	0.79	0.72	0.72
SSFIp	0.79	0.72	0.76	0.74	0.76	0.78	0.74	0.75
SPIe	0.81	0.72	0.77	0.74	0.83	0.81	0.73	0.72
SSFIe	0.79	0.75	0.73	0.77	0.77	0.80	0.73	0.73

To investigate the statistical significance of the correlation analysis between the MSDI and single-variable indices at the 12-month timescale, p-values were computed. These p-values assess the statistical significance of the observed correlations between the two continuous variables within the framework of Pearson correlation analysis. The p-values for the correlation analysis are shown in Table 4.

The results indicated that all observed correlations yielded exceptionally small p-values, suggesting that the likelihood of these correlations occurring by chance is virtually negligible. This finding underscores the robustness of the relationships identified in the analysis.

Different types of droughts may occur at different times for a given time frame. Occurrence of a specific drought type such as meteorological does not necessarily mean the occurrence of a drought in an integrated manner (Zhang et al. 2019). Hence, multivariate analysis of drought can capture drought events that single variable indices cannot. Consequently, combining multiple aspects of drought into a comprehensive drought index holds substantial importance for drought monitoring and mitigation.

Given its reliability, ease of calculation, and effectiveness, the MSDI is a superior tool for accurately representing drought conditions within an integrated framework. MSDI accurately represents actual drought conditions, making it an invaluable asset for drought assessment and management.

4.2 Drought characteristics in the SRB

In this study, a drought event occurs when MSDI values remain below −0.8 for more than three consecutive months. The area is considered fully recovered from drought once the MSDI values exceed −0.2 (Mo 2011). The time period between the full recovery of the affected area and the end of the drought is referred to as the termination period of the drought.

After examining the MSDI values for the entire basin, dry periods were observed in 1989–1990, 1993, 2005–2006 and 2007–2009 (Fig. 3). The longest dry period for the SRB spanned from 2007 to 2009 for all time scales. It is evident from Fig. 3 that although single

Table 4 *p* values of the correlation analysis between the MSDI and single variable indices at 12-month time scale

Index	D18A008	D18A012	D18A023	D18A027	E1801	E1805	E1820	E1825
SPIp	2.37e−61	1.49e−44	2.67e−54	7.06e−45	2.57e−59	6.72e−58	5.28e−44	1.54e−43
SSFIp	4.50e−58	3.94e−44	9.42e−51	1.70e−47	2.49e−50	9.52e−55	3.59e−47	2.73e−48
SPIe	3.59e−62	1.27e−43	3.98e−53	1.43e−46	1.48e−68	1.06e−63	2.46e−45	1.45e−43
SSFIe	6.53e−59	1.74e−49	1.77e−44	4.50e−53	7.13e−53	2.80e−59	5.75e−46	4.41e−45

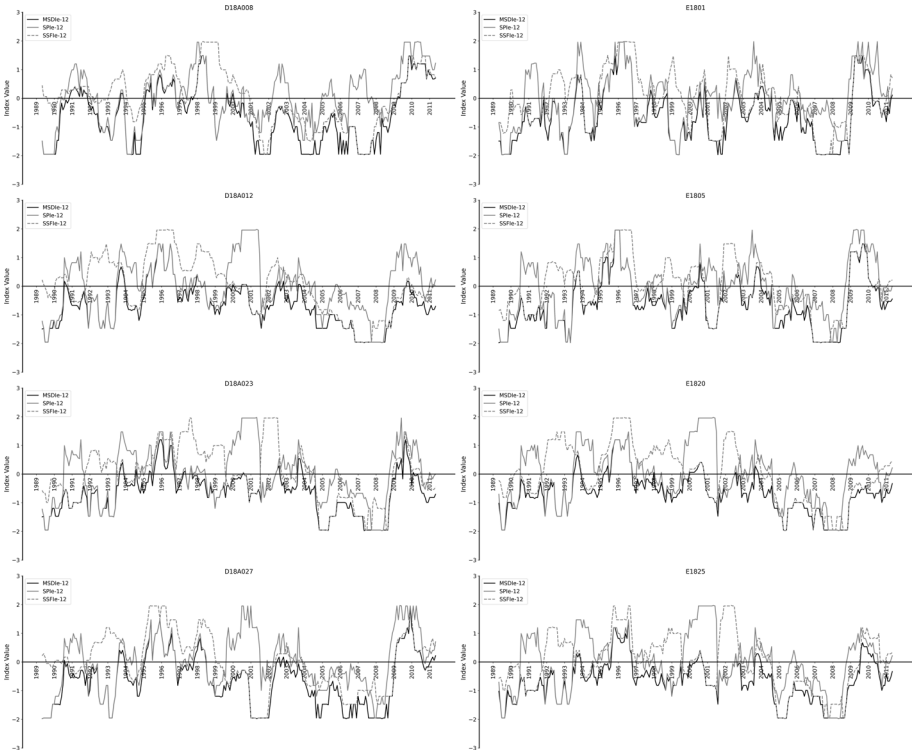

Fig. 3 Calculated indices from 1989 to 2011 for the 12-month time scale for all the stations in the SRB

variable indices captured some of the observed dry periods, they were unable to capture all of them, as they can only assess one type of drought. Conversely, the MSDI accurately captured dry periods for both meteorological and hydrological drought, owing to its integrated evaluation approach.

At station D18A027, multiple different drought events have been identified at 12-month time scale for MSDI, with the longest event extending to 40 months.

Drought characteristics, and the frequency of occurrence for drought events have been calculated for both single variable indices and the MSDI across all time scales. For simplicity only the results for D18A027 station at 12-month time scale are presented in Table 5.

According to the MSDI-12 calculations, there are several significant drought events between 1989 and 2008. Notably, the longest drought lasted 40 months, beginning in January 2006, with a severity of −65.05. This drought event was both the longest and most severe, underlining the intensity of drought conditions within that period. In contrast, SPI-12 indices reveal a series of shorter droughts with the longest single event lasting only 14 months and reaching a severity of −22.07. While MSDI-12 generally captures longer durations and greater severity in its drought assessments, the SPI-12 indices show more frequent, shorter droughts, indicating a divergence in drought type and severity detection between the two indices.

Similarly, the SSFI-12 index shows multiple drought events, with the longest recorded at 22 months starting in May 2006, with a severity of −26.69. These differences highlight

Table 5 Drought characteristics of single variable indices and the MSDI for D18A027 in the SRB

Index	Start date	Duration (month)	Severity	Frequency of occurrence	Recovery duration (month)
MSDI-12	Sep.89	15	− 24.57	5.66	2
	Feb.92	1	− 0.82	0.38	No recovery
	Apr.92	2	− 2.19	0.75	2
	Nov.92	12	− 17.00	4.53	2
	Oct.94	1	− 0.82	0.38	No recovery
	Jan.95	3	− 3.38	1.13	2
	Apr.97	1	− 0.82	0.38	2
	Jan.99	1	− 0.82	0.38	No recovery
	Mar.99	10	− 10.66	3.77	No recovery
	Feb.00	2	− 1.81	0.75	No recovery
	Apr.01	16	− 28.88	6.04	3
	Jun.04	18	− 23.77	6.79	No recovery
	Jan.06	40	− 65.05	15.09	No recovery
SPI-12	Sep.89	14	− 22.07	5.28	2
	Apr.92	1	− 1.20	0.38	2
	Nov.92	12	− 17.00	4.53	2
	Feb.95	1	− 0.82	0.38	2
	Jan.99	1	− 0.82	0.38	No recovery
	Mar.99	1	− 0.82	0.38	No recovery
	May.99	4	− 3.66	1.51	5
	Dec.01	1	− 0.99	0.38	4
	Nov.04	1	− 0.82	0.38	No recovery
	Jan.05	9	− 8.98	3.40	2
	Oct.06	1	− 0.99	0.38	2
	Nov.07	14	− 19.16	5.28	No recovery
SSFI-12	Feb.00	2	− 1.64	0.75	No recovery
	Apr.01	15	− 26.76	5.66	2
	Jul.04	7	− 5.77	2.64	No recovery
	Mar.05	2	− 1.81	0.75	No recovery
	May.06	22	− 26.69	8.30	No recovery
	May.08	12	− 14.66	4.53	No recovery

the varying perspectives provided by each drought index, where MSDI-12 appears to offer a broader drought assessment, potentially capturing both meteorological and hydrological conditions more comprehensively than SPI-12 and SSFI-12.

As the time scale increases, drought duration generally extends, although the frequency of drought occurrences diminishes. This behavior is consistent across different drought indices, which, despite some variations in their specific results, support a similar trend. These results, specifically from station D18A027 in the SRB, align closely with findings from other stations in the region, emphasizing that relying on a single-variable index may limit the understanding of complex drought dynamics.

4.3 Trend analysis of MSDI in the SRB

The trends of MSDI from 1989 to 2011 were analyzed using the Modified Mann–Kendall method (Hamed and Rao 1998), as correlation analysis revealed notable autocorrelation within the MSDI series. The MSDI showed no significant trend at %99 confidence level in the SRB (Table 6.).

To further explore the factors influencing this result, we analyzed the trends of precipitation and streamflow separately across the basin. Precipitation data exhibited no statistically significant trends at any of the meteorological stations, consistent with the lack of trend observed in SPI-12 assessments. Streamflow data, however, indicated a significant decreasing trend at five out of eight hydrological stations, while SSFI-12 assessments showed decreasing trends at only two of these stations. These findings suggest that the MSDI's lack of a significant trend is a result of the contrasting behaviors of precipitation and streamflow trends, which offset one another in the integrated analysis.

This outcome underscores the role of MSDI in providing a holistic assessment of drought conditions at the basin scale. While single-variable indices like SSFI are valuable for assessing trends in individual components, they may not fully capture the interplay between meteorological and hydrological processes that define drought dynamics. MSDI, in contrast, avoids overemphasis on localized trends in individual variables and provides a broader perspective on basin-wide drought characteristics.

4.4 Relationship between ENSO indices and the MSDI

In the present study, Nino 3.4, sunspot activities, and the Arctic Oscillation (AO) were selected to investigate the relationships between ENSO events and the MSDI series in the SRB, with the analysis conducted on an annual scale.

Figure 4 shows the wavelet correlation map of the Nino 3.4 index and the MSDI series over a period from 1989 to 2011. Upon examination of the graph, it is observed that the wavelet power spectrum, indicated by the color gradient, shows zones of significant covariance between the indices, especially notable at the 32-month period band. Within these zones, the arrows provide a directional cue to the phase relationship. A majority of rightward-pointing arrows within significant power regions suggest periods when ENSO and drought conditions, as quantified by the MSDI, are positively correlated, peaking and troughing in unison.

For instance, the swath of rightward arrows across the middle of the graph, especially pronounced in the late 1990s through the early 2000s, may indicate a consistent in-phase relationship where ENSO events align with the MSDI. This suggests that during these periods, phases of the ENSO cycle such as El Niño or La Niña could be linked with corresponding shifts in drought conditions.

Conversely, areas with leftward-pointing arrows, such as those sporadically observed in the early 1990s, signify periods where the phase relationship between Nino 3.4 and MSDI is inverse. During these times, the peaking of one index corresponds with the troughing of

Table 6 The Z values of MMK of annual MSDI in each station from 1989 to 2011

	E1801	E1805	E1820	E1825	D18A008	D18A012	D18A023	D18A027
Z value	0.72	0.56	− 1.13	− 0.25	− 0.17	− 1.16	− 0.18	− 0.26

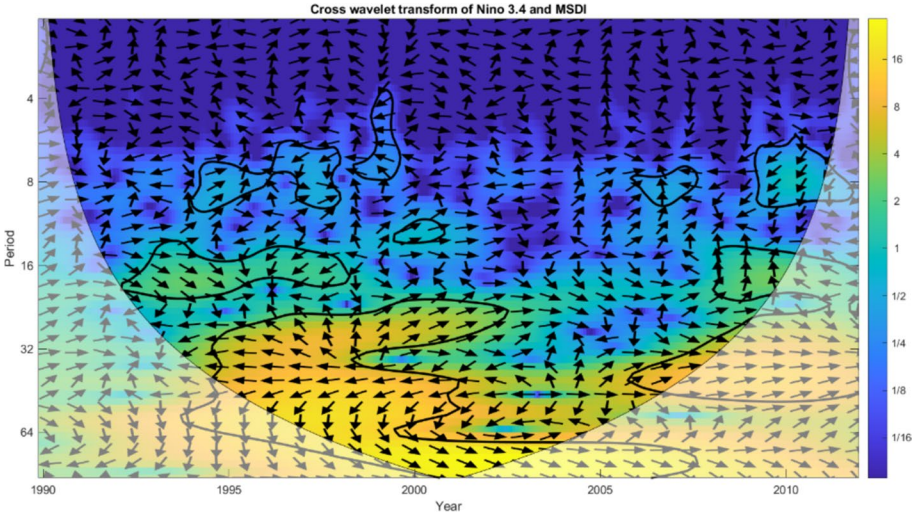

Fig. 4 Wavelet correlation map of Nino 3.4 and the MSDI

the other, indicating an anti-phase relationship where, for example, warm ENSO events might align with less severe drought conditions or vice versa.

The presence of both in-phase and anti-phase relationships within the graph highlights the complex and non-stationary nature of the interaction between oceanic-atmospheric dynamics and terrestrial hydrological responses. The findings underscore the variable influence of ENSO on drought patterns, which can fluctuate not only in intensity but also in the nature of their temporal alignment.

Figure 5 shows the wavelet correlation map of the AO and the MSDI series. Upon examining the graph, the predominance of leftward-pointing arrows should be noted.

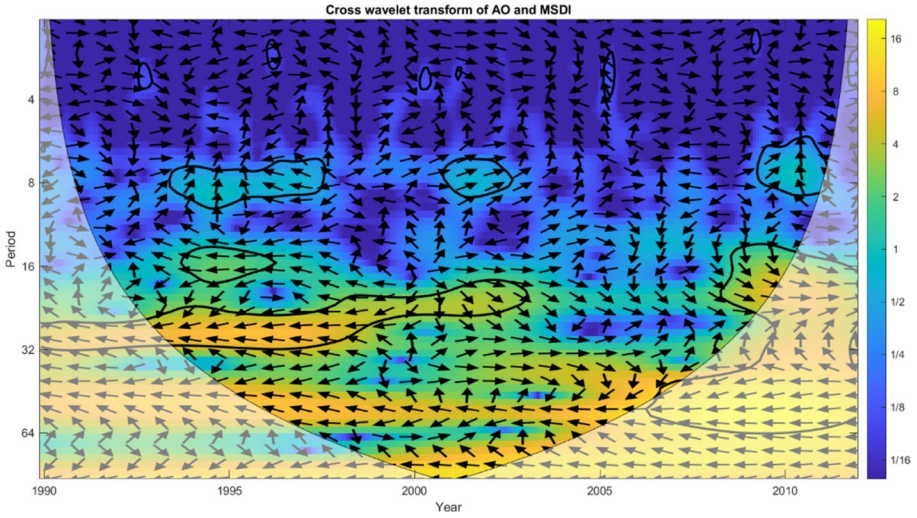

Fig. 5 Wavelet correlation map of the AO and the MSDI

These arrows suggest that, for much of the time period under study, there appears to be a predominantly anti-phase relationship between the AO and MSDI.

The high concentration of anti-phase arrows in the regions with significant wavelet power, especially at the 32-month band, strengthens the suggestion of a robust inverse relationship. These findings suggest a consistent anti-phase linkage over mid-term periods, signifying that oscillations in the AO are likely reflected inversely in hydrological conditions, as captured by the MSDI, with potential implications for regional climate and drought forecasting.

Figure 6 shows the wavelet correlation map of sunspot activity and the MSDI series. Upon examining the graph, there's a notable area, especially from early 1990s to the mid-2000s, with a high concentration of leftward-pointing arrows within the region of significant power at the 64 month period band. This suggests that during this time, high sunspot activity is inversely related to the conditions indicated by the MSDI. This could be interpreted as periods of high solar activity correlating with more severe drought conditions, or alternatively, low solar activity correlating with less severe drought conditions.

To conclude, the cross-wavelet analysis between sunspot activity and the MSDI over the studied period suggests an inverse relationship at mid-term frequencies, particularly within the 32–64 month period band. This inverse relationship indicates that periods of heightened solar activity may be associated with more intense drought conditions as measured by the MSDI, or the opposite. This analysis contributes to the broader understanding of how extraterrestrial factors, such as solar variability, can potentially interact with and influence terrestrial hydrological processes and climatic conditions in the SRB.

4.5 Comparison between single variable indices and the MSDI

The correlation coefficients between the SPI and the SSFI ranged from 0.17 to 0.35 across all time scales. These correlation coefficients increased significantly when comparing the SPI with the MSDI, with values ranging between 0.74 and 0.83. Similarly, the correlation coefficients between SSFI and MSDI varied from 0.66 to 0.77. Notably, the relationship

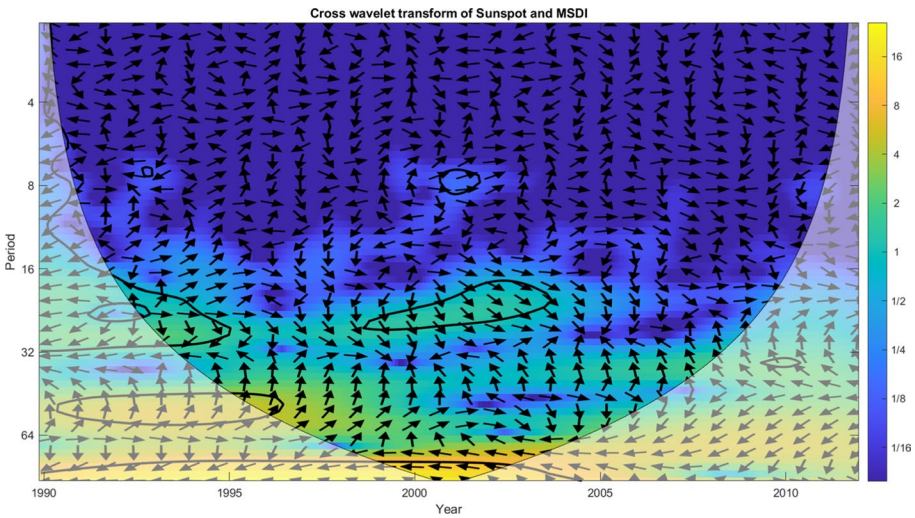

Fig. 6 Wavelet correlation map of the Sunspots and the MSDI

between SPI and SSFI was significantly weaker than that observed between these indices and the MSDI across all timescales. An improvement in correlation between single variable indices is visible when transitioning from single variable indices to the MSDI (Yisehak and Zenebe 2020).

The coefficient of determination was utilized to further investigate the relationship between the single variable indices and the MSDI. As seen in Fig. 7, the MSDI demonstrated a relationship with an R^2 value exceeding 0.5 across nearly all timescales when compared with both parametric and empirical single variable indices. Although only the

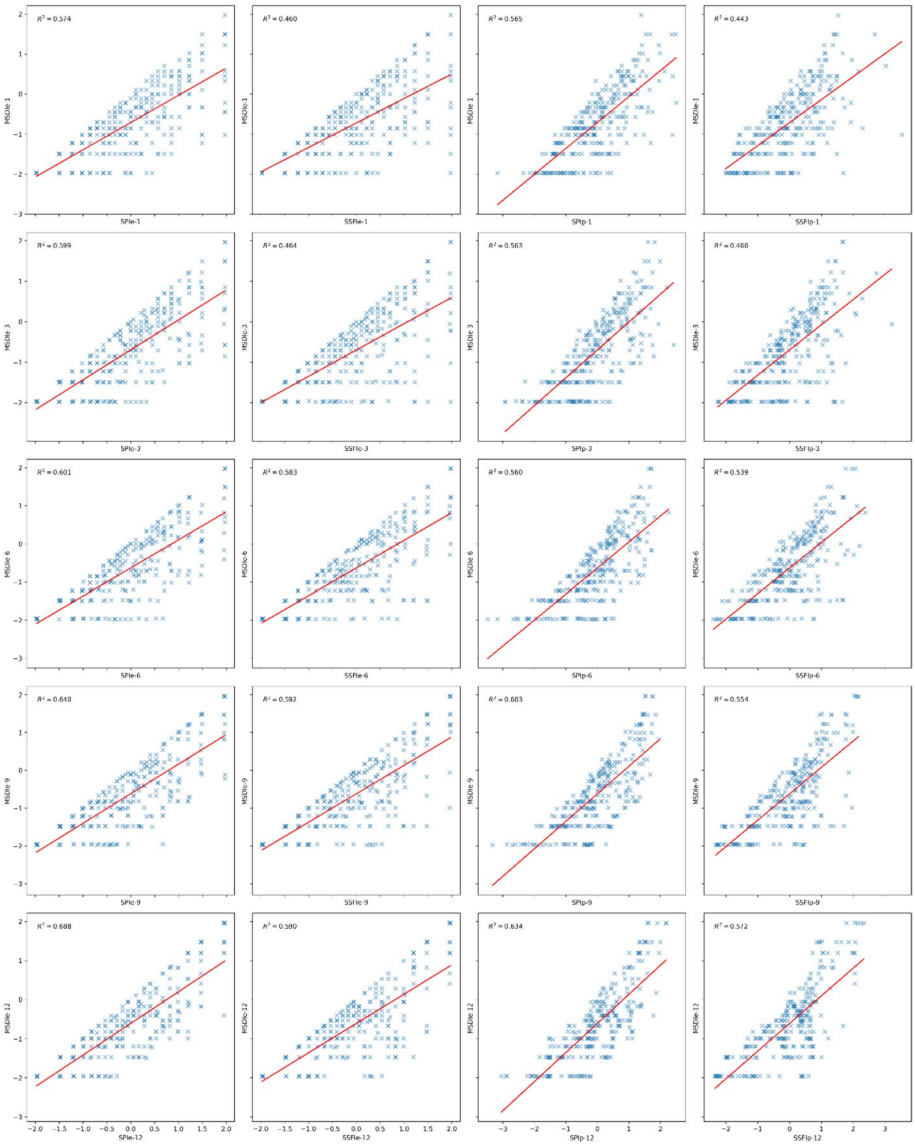

Fig. 7 Regression equations between single variable indices and the MSDI at E1801

results for E1801 are presented in Fig. 7, similar results were observed across all stations. Significance values are presented in Table 7.

The p-values presented in Table 7. are exceptionally small, indicating that the observed relationships are highly statistically significant. This suggests a strong and consistent connection between the MSDI and the indices, with minimal likelihood that these relationships are due to chance. Notably, the significance values tend to decrease with increasing timescale, particularly for the SPIp and SPIe indices, highlighting that the relationship between the MSDI and these indices strengthens over longer time periods.

5 Discussion

The present study developed and applied a nonparametric standardized multivariate drought index to characterize drought conditions in the SRB, integrating both meteorological and hydrological variables. The results indicate that MSDI is effective in capturing the complex drought dynamics of the SRB, which features Mediterranean climate characteristics and significant seasonal variability. Compared to traditional single-variable indices, such as the SPI and the SSFI, the MSDI provided a more holistic drought assessment, identifying events with greater sensitivity across multiple time scales.

MSDI offers several advantages as a comprehensive tool for drought monitoring and assessment. Its nonparametric nature makes it highly adaptable to various datasets, avoiding the need for strict assumptions about data distributions, which is particularly useful in regions with limited or variable data. Compared to parametric methods, the MSDI is easier to calculate, as it does not require complex statistical assumptions or fitting of specific distribution models. The index captures a broad range of drought conditions, including meteorological and hydrological droughts, providing a multi-dimensional understanding of drought events. Additionally, the MSDI is sensitive to both short-term fluctuations and long-term drought trends, offering flexibility for detecting different phases and intensities of drought.

Despite the advantages, there are limitations to the nonparametric MSDI approach. The method is sensitive to data record length and quality, which may limit its applicability in regions with shorter hydrological records or incomplete datasets. A sensitivity analysis on record length showed that while the drought index generally maintained consistent patterns across different periods, shorter records were more sensitive to short-term variability. Additionally, shorter records exhibited more variability in the distribution of index values, especially in the extremes, and showed less stability in capturing the full range of drought conditions. Longer records, on the other hand, provided a more stable and reliable representation of drought trends and extremes.

The findings from this study highlight the value of adopting a multivariate, nonparametric approach to drought monitoring in regions prone to significant seasonal variability

Table 7 Significance values of the relationship between MSDI and single variable indices across different time scales

Index	1-month	3-month	6-month	9-month	12-month
SPIp	1.91E−51	9.41E−51	6.16E−50	2.86E−55	2.57E−59
SSFIp	1.21E−36	3.12E−38	3.61E−47	1.38E−48	2.49E−50
SPIe	1.19E−52	6.79E−56	1.17E−55	5.15E−61	1.47E−68
SSFIe	1.45E−38	1.16E−38	3.61E−47	1.01E−53	7.13E−53

and water scarcity. By combining meteorological and hydrological data, MSDI provides a comprehensive view of drought conditions that can be used to support water resource management decisions. This approach is especially useful for agricultural and municipal water planning, as it can help forecast and mitigate the effects of prolonged dry periods. In the Seyhan River Basin, where water availability is critical for agriculture and energy production, MSDI's robust assessment of drought conditions can support proactive drought management strategies.

Future work could focus on incorporating datasets with longer record periods to improve the accuracy of drought assessments, as extended data would provide a more reliable representation of long-term trends. Additionally, integrating soil moisture data into the MSDI calculation could enhance its robustness, leading to the development of an all-encompassing MSDI that captures hydrological, meteorological, and agricultural drought conditions. This comprehensive approach would not only provide a more holistic understanding of drought but also offer a tool that is easier for policymakers to interpret and act upon, enabling more effective and timely drought management strategies.

6 Conclusion

The present study employs a nonparametric method that integrates meteorological and hydrological types of droughts. As it is mentioned in Sect. 2.1, the SRB is prone to drought and has been extensively studied in the literature. However, existing literature lacks comprehensive multivariate analyses of drought in the SRB. This study employs MSDI to investigate the drought situation from a multivariate perspective in the SRB from 1989 to 2011. The MSDI is distribution-independent and addresses the limitations inherent in prior parametric approaches. Furthermore, the cross-wavelet correlation technique was utilized to investigate the relationships between ENSO indices and the MSDI in the SRB. The key findings of this study are as follows:

(1) MSDI shows a strong correlation with SPI and SSFI in all time scales, confirming the effectiveness of the nonparametric method in reliably characterizing drought conditions within the SRB. The integration of both precipitation and streamflow data by the MSDI enhances its effectiveness in characterizing drought in an integrated manner compared to single-variable indices.
(2) An insubstantial negative trend was detected in the MSDI for the SRB, suggesting an insignificant increase in drought severity over the period from 1989 to 2010.
(3) The most prolonged drought event within the SRB was recorded from 2006 to 2009 across all temporal scales, with durations extending to 50 months at certain stations for the 12-month time scale. Additional prominent drought occurrences were identified in the years 1989 to 1990, in 1993, and from 2005 to 2006. The MSDI demonstrated heightened sensitivity and reliability in the integrated detection of these drought events compared to single variable indices.
(4) While peripheral to the primary aim of our research, we observed notable disparities in the distribution tails of parametric and empirical single variable indices. This divergence likely stems from the dependency of parametric indices on specific distribution parameters, which necessitate precise estimations.
(5) The progression of drought within the SRB displayed a discernible relationship with the Nino 3.4 and Arctic Oscillation indices. The MSDI and Nino 3.4 indices predomi-

nantly exhibited a synchronous relationship, whereas the Arctic Oscillation and MSDI frequently revealed an inverse relationship.

(6) This study scrutinized the correlation between single variable indices and the MSDI. The findings indicate that the relationship between the SPI and the SSFI was enhanced concomitantly with the development of the MSDI.

Funding Open access funding provided by the Scientific and Technological Research Council of Türkiye (TÜBİTAK). Not applicable.

Data availability The datasets used and/or analyzed during the current study are available from the corresponding author on reasonable request.

Code availability Not applicable.

Declarations

Conflict of interest All authors certify that they have no affiliations with or involvement in any organization or entity with any financial interest or non-financial interest in the subject matter or materials discussed in this manuscript. The authors declare that they have no conflicts of interest. None of the authors have any competing interests in the manuscript. The authors declare that they have no known competing financial interests.

Ethical of approval Not applicable.

Consent for publication Not applicable.

References

AghaKouchak A, Cheng L, Mazdiyasni O, Farahmand A (2014) Global warming and changes in risk of concurrent climate extremes: Insights from the 2014 California Drought. Geophys Res Lett 41(24):8847–8852. https://doi.org/10.1002/2014gl062308

AghaKouchak A, Chiang F, Huning LS, Love CA, Mallakpour I, Mazdiyasni O, Moftakhari H, Papalexiou SM, Ragno E, Sadegh M (2020) Climate extremes and compound hazards in a warming world. Annu Rev Earth Planet Sci 48(1):519–548

Ahmadi B, Ahmadalipour A, Moradkhani H (2019) Hydrological drought persistence and recovery over the CONUS: a multi-stage framework considering water quantity and quality. Water Res 150:97–110. https://doi.org/10.1016/j.watres.2018.11.052

Ali M, Deo RC, Maraseni T, Downs NJ (2019) Improving SPI-derived drought forecasts incorporating synoptic-scale climate indices in multi-phase multivariate empirical mode decomposition model hybridized with simulated annealing and kernel ridge regression algorithms. J Hydrol 576:164–184. https://doi.org/10.1016/j.jhydrol.2019.06.032

Altın TB, Sarış F, Altın BN (2019) Determination of drought intensity in Seyhan and Ceyhan river basins, Turkey, by hydrological drought analysis. Theoret Appl Climatol 139(1–2):95–107. https://doi.org/10.1007/s00704-019-02957-y

American Meteorological Society (2004) Statement on meteorological drought. Bull Am Meteor Soc 85:771–773

Angelidis P, Maris F, Kotsovinos N, Hrissanthou V (2012) Computation of drought index SPI with alternative distribution functions. Water Resour Manage 26(9):2453–2473. https://doi.org/10.1007/s11269-012-0026-0

Aon S, Biswas S (2023) Spatially distributed Bivariate Meteorological Drought Analysis using copula technique in a semi-arid river basin of West Bengal, India. Theor Appl Climatol 155(4):2885–2901. https://doi.org/10.1007/s00704-023-04790-w

Aon S, Biswas S (2024) Bivariate Assessment of Hydrological Drought of a semi-arid basin and investigation of drought propagation using a novel cross wavelet transform based technique. Water Resour Manage 38(8):2977–3005. https://doi.org/10.1007/s11269-024-03801-3

Aon S, Nandi S, Sen S, Biswas S (2024) Grace based groundwater drought evaluation of Ganga Basin and analysis of drought propagation using wavelet based quantitative approach. Sci Total Environ 951:175666. https://doi.org/10.1016/j.scitotenv.2024.175666

Carlson TN, Gillies RR, Perry EM (1994) A method to make use of thermal infrared temperature and NDVI measurements to infer surface soil water content and fractional vegetation cover. Remote Sens Rev 9(1–2):161–173. https://doi.org/10.1080/02757259409532220

Cavus Y, Aksoy H (2019) Spatial drought characterization for Seyhan River basin in the Mediterranean region of Turkey. Water 11(7):1331. https://doi.org/10.3390/w11071331

Cavus Y, Stahl K, Aksoy H (2023) Drought intensity–duration–frequency curves based on deficit in precipitation and streamflow for water resources management. Hydrol Earth Syst Sci 27(18):3427–3445. https://doi.org/10.5194/hess-27-3427-2023

Crausbay SD, Ramirez AR, Carter SL, Cross MS, Hall KR, Bathke DJ, Betancourt JL, Colt S, Cravens AE, Dalton MS, Dunham JB, Hay LE, Hayes MJ, McEvoy J, McNutt CA, Moritz MA, Nislow KH, Raheem N, Sanford T (2017) Defining ecological drought for the twenty-first century. Bull Am Meteor Soc 98(12):2543–2550. https://doi.org/10.1175/bams-d-16-0292.1

Dikici M (2022) Drought analysis for the Seyhan Basin with vegetation indices and comparison with meteorological different indices. Sustainability 14:4464. https://doi.org/10.3390/su14084464

Dracup JA, Lee KS, Paulson EG (1980) On the definition of droughts. Water Resour Res 16(2):297–302. https://doi.org/10.1029/wr016i002p00297

Fang W, Huang S, Huang Q, Huang G, Meng E, Luan J (2018) Reference evapotranspiration forecasting based on local meteorological and global climate information screened by Partial Mutual Information. J Hydrol 561:764–779. https://doi.org/10.1016/j.jhydrol.2018.04.038

Fang W, Huang S, Huang Q, Huang G, Wang H, Leng G, Wang L, Li P, Ma L (2019) Bivariate probabilistic quantification of drought impacts on terrestrial vegetation dynamics in Mainland China. J Hydrol 577:123980. https://doi.org/10.1016/j.jhydrol.2019.123980

Farahmand A, AghaKouchak A (2015) A generalized framework for deriving nonparametric standardized drought indicators. Adv Water Resour 76:140–145. https://doi.org/10.1016/j.advwatres.2014.11.012

Gringorten II (1963) A plotting rule for extreme probability paper. J Geophys Res 68(3):813–814. https://doi.org/10.1029/jz068i003p00813

Grinsted A, Moore JC, Jevrejeva S (2004) Application of the cross wavelet transform and wavelet coherence to Geophysical Time Series. Nonlinear Process Geophys 11(5/6):561–566. https://doi.org/10.5194/npg-11-561-2004

Gumus V (2023) Evaluating the effect of the SPI and SPEI methods on drought monitoring over Turkey. J Hydrol 626:130386. https://doi.org/10.1016/j.jhydrol.2023.130386

Gumus V, Algin HM (2016) Meteorological and hydrological drought analysis of the seyhan−ceyhan river basins, Turkey. Meteorol Appl 24(1):62–73. https://doi.org/10.1002/met.1605

Guttman NB (1999) Accepting the standardized precipitation index: a calculation algorithm[1]. JAWRA J Am Water Resourc Assoc 35(2):311–322. https://doi.org/10.1111/j.1752-1688.1999.tb03592.x

Hamed KH, Ramachandra RA (1998) A modified Mann-Kendall trend test for autocorrelated data. J Hydrol 204(1–4):182–196. https://doi.org/10.1016/s0022-1694(97)00125-x

Hao Z, AghaKouchak A (2013) Multivariate standardized drought index: a parametric multi-index model. Adv Water Resour 57:12–18. https://doi.org/10.1016/j.advwatres.2013.03.009

Hao Z, AghaKouchak A (2014) A nonparametric multivariate multi-index drought monitoring framework. J Hydrometeorol 15(1):89–101. https://doi.org/10.1175/jhm-d-12-0160.1

Hao Z, Hao F, Singh VP, Ouyang W, Cheng H (2017) An integrated package for drought monitoring, prediction and analysis to aid drought modeling and assessment. Environ Model Softw 91:199–209. https://doi.org/10.1016/j.envsoft.2017.02.008

Hayes MJ, Svoboda MD, Wilhite DA, Vanyarkho OV (1999) Monitoring the 1996 drought using the standardized precipitation index. Bull Am Meteor Soc 80(3):429–438. https://doi.org/10.1175/1520-0477(1999)080%3c0429:MTDUTS%3e2.0.CO;2

Heudorfer B, Stahl K (2016) Comparison of different threshold level methods for drought propagation analysis in Germany. Hydrol Res 48(5):1311–1326. https://doi.org/10.2166/nh.2016.258

Huang S, Chang J, Huang Q, Chen Y (2014a) Identification of abrupt changes of the relationship between rainfall and runoff in the Wei River Basin, China. Theor Appl Climatol 120(1–2):299–310. https://doi.org/10.1007/s00704-014-1170-7

Huang S, Chang J, Huang Q, Chen Y (2014b) Spatio-temporal changes and frequency analysis of drought in the Wei River Basin, China. Water Resourc Manage 28(10):3095–3110. https://doi.org/10.1007/s11269-014-0657-4

Huang S, Huang Q, Chang J, Leng G (2015) Linkages between hydrological drought, climate indices and human activities: a case study in the Columbia River Basin. Int J Climatol 36(1):280–290. https://doi.org/10.1002/joc.4344

Huang S, Huang Q, Leng G, Chang J (2016) A hybrid index for characterizing drought based on a nonparametric kernel estimator. J Appl Meteorol Climatol 55(6):1377–1389. https://doi.org/10.1175/jamc-d-15-0295.1

Huang S, Wang L, Wang H, Huang Q, Leng G, Fang W, Zhang Y (2019) Spatio-temporal characteristics of drought structure across China using an integrated drought index. Agric Water Manag 218:182–192. https://doi.org/10.1016/j.agwat.2019.03.053

IPCC (2012) Managing the risks of extreme events and disasters to advance climate change adaptation. Cambridge University Press, Cambridge

Kao S-C, Govindaraju RS (2010) A copula-based joint deficit index for droughts. J Hydrol 380(1–2):121–134. https://doi.org/10.1016/j.jhydrol.2009.10.029

Kendall MG (1955) Rank correlation methods. Charles Griffin, London

Keyantash J, Dracup JA (2002) The quantification of drought: an evaluation of drought indices. Bull Am Meteor Soc 83(8):1167–1180. https://doi.org/10.1175/1520-0477-83.8.1167

Keyantash JA, Dracup JA (2004) An aggregate drought index: assessing drought severity based on fluctuations in the hydrologic cycle and surface water storage. Water Resourc Res 40:2003WR002610. https://doi.org/10.1029/2003WR002610

Lee S, Moriasi DN, Danandeh Mehr A, Mirchi A (2024) Sensitivity of standardized precipitation and Evapotranspiration index (SPEI) to the choice of spei probability distribution and evapotranspiration method. J Hydrol Reg Stud 53:101761. https://doi.org/10.1016/j.ejrh.2024.101761

Liu X, Zhu X, Pan Y, Li S, Liu Y, Ma Y (2016a) Agricultural drought monitoring: progress, challenges, and prospects. J Geog Sci 26(6):750–767. https://doi.org/10.1007/s11442-016-1297-9

Liu Z, Wang Y, Shao M, Jia X, Li X (2016b) Spatiotemporal analysis of multiscalar drought characteristics across the Loess Plateau of China. J Hydrol 534:281–299. https://doi.org/10.1016/j.jhydrol.2016.01.003

Liu Y, Ding Z, Chen Y, Yan F, Yu P, Man W, Liu M, Li H, Tang X (2023) Restored vegetation is more resistant to extreme drought events than natural vegetation in southwest China. Sci Total Environ 866:161250. https://doi.org/10.1016/j.scitotenv.2022.161250

Luo Y, Liu Y, Dong Z, Li Q, Zhang X, Dong X (2023) Development of multivariate standardized drought index for Large Lake basins based on the copula function: a case study of Hongze Lake Basin, China. J Hydrol Reg Stud 50:101586. https://doi.org/10.1016/j.ejrh.2023.101586

Mann HB (1945) Nonparametric tests against trend. Econometrica 13(3):245. https://doi.org/10.2307/1907187

McKee TB, Doesken NJ, Kleist J (1993) The relationship of drought frequency and duration to time scales. In: 8th Conference on applied climatology, Anaheim, CA, January 17–22, 1993, pp 179–184

Ministry of Forestry and Water Affairs, General Directorate of Water Management (GDWM), Flood and Drought Management Department. (2019). Seyhan basin drought management plan: final report, executive summary. Ankara, Turkey

Mishra AK, Singh VP (2010) A review of drought concepts. J Hydrol 391(1–2):202–216. https://doi.org/10.1016/j.jhydrol.2010.07.012

Mishra AK, Singh VP (2011) Drought modeling – a Review. J Hydrol 403(1–2):157–175. https://doi.org/10.1016/j.jhydrol.2011.03.049

Mo KC (2011) Drought onset and recovery over the United States. J Geophys Res 116(D20):16168. https://doi.org/10.1029/2011jd016168

Modarres R (2006) Streamflow drought time series forecasting. Stoch Env Res Risk Assess 21(3):223–233. https://doi.org/10.1007/s00477-006-0058-1

Mukhawana MB, Kanyerere T, Kahler D, Masilela NS, Lalumbe L, Umunezero AA (2024) Hydrological drought assessment using the standardized groundwater index and the standardized precipitation index in the Berg River catchment, South Africa. J Hydrol Reg Stud 53:101779. https://doi.org/10.1016/j.ejrh.2024.101779

Nalbantis I, Tsakiris G (2008) Assessment of hydrological drought revisited. Water Resour Manage 23(5):881–897. https://doi.org/10.1007/s11269-008-9305-1

Narasimhan B, Srinivasan R (2005) Development and evaluation of soil moisture deficit index (SMDI) and Evapotranspiration Deficit index (ETDI) for Agricultural Drought Monitoring. Agric for Meteorol 133(1–4):69–88. https://doi.org/10.1016/j.agrformet.2005.07.012

Naresh Kumar M, Murthy CS, Sesha Sai MV, Roy PS (2009) On the use of standardized precipitation index (SPI) for Drought intensity assessment. Meteorol Appl 16(3):381–389. https://doi.org/10.1002/met.136

Önöz B, Bayazit M (2003) The power of statistical tests for trend detection. Turk J Eng Environ Sci 27(4):247–251

Panu US, Sharma TC (2002) Challenges in drought research: some perspectives and future directions. Hydrol Sci J 47(sup1):S19–S30. https://doi.org/10.1080/02626660209493019

Pascolini-Campbell M, Reager JT, Chandanpurkar HA et al (2021) RETRACTED ARTICLE: a 10 per cent increase in global land evapotranspiration from 2003 to 2019. Nature 593:543–547. https://doi.org/10.1038/s41586-021-03503-5

Quiring SM (2009) Developing objective operational definitions for Monitoring Drought. J Appl Meteorol Climatol 48(6):1217–1229. https://doi.org/10.1175/2009jamc2088.1

Reidmiller DR, Avery CW, Easterling DR, Kunkel KE, Lewis KLM et al (eds) (2018) Impacts, risks, and adaptation in the United States: The Fourth National Climate Assessment. US Global Change Research Program, USA

Seo J, Won J, Lee H, Kim S (2024) Probabilistic monitoring of meteorological drought impacts on water quality of major rivers in South Korea using copula models. Water Res 251:121175. https://doi.org/10.1016/j.watres.2024.121175

Shafer BA, Dezman LE (1982) Development of surface water supply index (SWSI) to assess the severity of drought condition in snowpack runoff areas. In: Proceeding of the western snow conference

Sharma A (2000) Seasonal to interannual rainfall probabilistic forecasts for improved water supply management: Part 3—a nonparametric probabilistic forecast model. J Hydrol 239(1–4):249–258. https://doi.org/10.1016/s0022-1694(00)00348-6

She D, Xia J (2017) Copulas-based drought characteristics analysis and risk assessment across the Loess Plateau of China. Water Resour Manage 32(2):547–564. https://doi.org/10.1007/s11269-017-1826-z

Smakhtin VU (2001) Low flow hydrology: A Review. J Hydrol 240(3–4):147–186. https://doi.org/10.1016/s0022-1694(00)00340-1

Su Yönetimi Genel Müdürlüğü (SYGM). (2019). *Seyhan Havzası Kuraklık Koruma Planı*. T.C. Tarım ve Orman Bakanlığı

Suo N, Xu C, Cao L, Song L, Lei X (2024) A copula-based parametric composite drought index for drought monitoring and applicability in arid Central Asia. CATENA 235:107624. https://doi.org/10.1016/j.catena.2023.107624

Svoboda M, LeComte D, Hayes M, Heim R, Gleason K, Angel J, Rippey B, Tinker R, Palecki M, Stooksbury D, Miskus D, Stephens S (2002) The drought monitor. Bull Am Meteor Soc 83(8):1181–1190. https://doi.org/10.1175/1520-0477-83.8.1181

Terzi TB, Önöz B (2024a) Çoruh havzasında meteorolojik kuraklıktan hidrojik kuraklığa yayılımının analizi. In: Proceedings of the XII. Ulusal Hidroloji Kongresi. Samsun Üniversitesi Yayınları, pp 152–164

Terzi TB, Önöz B (2024) Drought analysis in the Seyhan River Basin based on standardized drought indices using a new approach considering seasonality. Environ Earth Sci. https://doi.org/10.1007/s12665-024-12039-6

Tijdeman E, Stahl K, Tallaksen LM (2020) Drought characteristics derived based on the standardized streamflow index: a large sample comparison for parametric and nonparametric methods. Water Resourc Res 56(10):2019WR026315. https://doi.org/10.1029/2019wr026315

Topçu E, Seçkin N, Haktanır NA (2021) Drought analyses of eastern Mediterranean, Seyhan, Ceyhan, and asi basins by using aggregate drought index (ADI). Theoret Appl Climatol 147(3–4):909–924. https://doi.org/10.1007/s00704-021-03873-w

Tripathy KP, Mishra AK (2023) How unusual is the 2022 European compound drought and Heatwave event? Geophys Res Lett 50(15):2023gl105453. https://doi.org/10.1029/2023gl105453

Van Loon AF, Laaha G (2015) Hydrological drought severity explained by climate and catchment characteristics. J Hydrol 526:3–14. https://doi.org/10.1016/j.jhydrol.2014.10.059

Varol T, Atesoglu A, Ozel HB, Cetin M (2023) Copula-based multivariate standardized drought index (MSDI) and length, severity, and frequency of hydrological drought in the Upper Sakarya Basin, Turkey. Nat Hazards 116:3669–3683. https://doi.org/10.1007/s11069-023-05830-4

Vicente-Serrano SM, Beguería S, López-Moreno JI (2010) A multiscalar drought index sensitive to global warming: The standardized precipitation Evapotranspiration index. J Clim 23(7):1696–1718. https://doi.org/10.1175/2009jcli2909.1

Walker DW, Van Loon AF (2023) Droughts are coming on faster. Science 380(6641):130–132. https://doi.org/10.1126/science.adh3097

Wang F, Wang Z, Yang H, Di D, Zhao Y, Liang Q, Hussain Z (2020) Comprehensive evaluation of hydrological drought and its relationships with meteorological drought in the Yellow River basin, China. J Hydrol 584:124751. https://doi.org/10.1016/j.jhydrol.2020.124751

Wang F, Lai H, Li Y, Feng K, Tian Q, Guo W, Qu Y, Yang H (2023) Spatio-temporal evolution and teleconnection factor analysis of groundwater drought based on the grace mascon model in the Yellow River Basin. J Hydrol 626:130349. https://doi.org/10.1016/j.jhydrol.2023.130349

Wilhite DA (2000) Drought as a natural hazard: concepts and definitions. In: Wilhite DA (ed) Droughts, 1st edn. Routledge. https://doi.org/10.4324/9781315830896

Wilhite DA (2005) Drought and water crises:science, technology, and management issues. CRC Press. https://doi.org/10.1201/9781420028386

Wilhite DA, Glantz MH (1985) Understanding: the drought phenomenon: the role of definitions. Water Int 10(3):111–120. https://doi.org/10.1080/02508068508686328

Wu J, An P, Zhao C, Wei Z, Lan T, Li X, Wang G (2024) Effects of multi-year droughts on the precipitation-runoff relationship: an integrated analysis of meteorological, hydrological, and compound droughts. J Hydrol 634:131064. https://doi.org/10.1016/j.jhydrol.2024.131064

Xu Y, Wang L, Ross K, Liu C, Berry K (2018) Standardized soil moisture index for drought monitoring based on soil moisture active passive observations and 36 years of North American Land Data assimilation system data: a case study in the Southeast United States. Remote Sens 10(2):301. https://doi.org/10.3390/rs10020301

Yisehak B, Zenebe A (2020) Modeling multivariate standardized drought index based on the drought information from precipitation and runoff: a case study of hare watershed of southern Ethiopian Rift Valley Basin. Model Earth Syst Environ 7(2):1005–1017. https://doi.org/10.1007/s40808-020-00923-6

Zhang D, Chen P, Zhang Q, Li X (2017) Copula-based probability of concurrent hydrological drought in the Poyang Lake-catchment-river system (China) from 1960 to 2013. J Hydrol 553:773–784. https://doi.org/10.1016/j.jhydrol.2017.08.046

Zhang Y, Huang S, Huang Q, Leng G, Wang H, Wang L (2019) Assessment of drought evolution characteristics based on a nonparametric and Trivariate Integrated Drought index. J Hydrol 579:124230. https://doi.org/10.1016/j.jhydrol.2019.124230

Zhu Y, Chang J, Huang S, Huang Q (2015) Characteristics of integrated droughts based on a nonparametric standardized drought index in the Yellow River Basin, China. Hydrol Res 47(2):454–467. https://doi.org/10.2166/nh.2015.287